Studies on Preparation of Immersion-Type Polypropylene Fragrant Fiber. I. Formation of Matrix Fiber in the Melt-Spinning Process and Its Technique of Immersion Essential Oil

Bing Wang, Jiasen Zhao

School of Material Science and Chemical Engineering, Tianjin Polytechnic University, Tianjin 300160, China

Received 23 August 2002; accepted 14 February 2003

ABSTRACT: Polypropylene/ethylene vinyl acetate (PP/EVA) blends were prepared in a plastic extruder with a static mixer. The thermodynamic compatibility, morphology, crystal form, and rheological behavior of PP/EVA blends were investigated by SEM, DSC, and rheology instruments. The results showed that PP and EVA were thermodynamically incompatible, the viscosity of the PP/EVA blends decreased with increase of shear rate in a range of temperature, the PP/EVA blends had a sea-islands structure, and the crystalline zones remained in their original state and could not form mixed crystals in the PP/EVA blends. The PP/EVA blends were melt spun to prepare matrix fibers and the spinning conditions such as EVA content, the matching factor between pump delivery and winding velocity, and the melt-spinning temperature were also determined. The sorption process of a matrix fiber for essential oils, adsorbed under various sorption conditions such as sorption time, sorption temperature, and EVA content, was also studied. The results revealed that the composite isotherm of the adsorption of matrix fiber for essential oil was characteristic of a *U* model. Through adsorbing essential oil, the immersion-type PP fragrant fibers could be prepared with the matrix fiber. © 2003 Wiley Periodicals, Inc. J Appl Polym Sci 90: 1970–1979, 2003

Key words: polypropylene (PP); blending; melt; fibers; adsorption

INTRODUCTION

In recent years, many kinds of fragrant textile products have been developed such as fragrant bat wool, fragrant handkerchief, fragrant curtain, and fragrant necktie. The experiments indicated that fragrant products may actually dispel a person's weariness, optimize the environment, disinfect, and diminish inflammation. The preparation technology of fragrant fibers stems from paintcoat technology of fragrant textiles. At present preparation of fragrant fibers is carried out with by the blending/spinning method.[1–7] The thermoplastic spin fiber-forming polymer and aromatics are blended with melt spinning by the extrusion method. In this process, the compatibility between aromatics and substrate material should be resolved. Because of limitations of the melt-spinning process, the boiling point of aromatics should be above 250°C. This means that the selection range of aromatics is quite narrow. The aromatics could be enclosed in a microcapsule to become a fragrant microcapsule. The fragrant microcapsules and thermoplastic fiber-forming polymers were mixed to spin the fragrant microcapsule fiber. The spicery was slowly released from the micropores in the wall materials of the microcapsule. The wall materials of the microcapsule were heat-resistant materials not only allowed the aromatics not to be heated directly in the spinning process but also prevented thermal decomposition. Although the selection range of aromatics was expanded, the wall materials and size of the microcapsule could significantly affect the spinning process.

We prepared high-quality fragrant fibers using an adsorbent in the matrix fiber to adsorb aromatics. Because the aromatics were not water soluble, the fragrant fiber had good laundry-resistant fastness. The aromatics did not participate in the process of high-temperature melt spinning, and thus the aromatics in the fiber could not volatilize easily, and the perfume of the fiber remained unchanged. In this study, we prepared a polypropylene/ethylene vinyl acetate (PP/EVA) blending fiber that could be then be used as the matrix of a polypropylene fragrant fiber by means of the melt-spinning method.[8–13]

EXPERIMENTAL

Main materials

Polypropylene [PP; melt flow index (MFI) = 17–18 g/min, melting temperature (T_m) = 171.18°C] was

Correspondence to: B. Wang (hxl_009@sina.com).

Journal of Applied Polymer Science, Vol. 90, 1970–1979 (2003)

supplied from Liaoyang Petroleum and Chemical Fiber Plant (China). Ethylene vinyl acetate resin [EVA; the content of VA was 30 ± 2% (determined by the saponification method), T_m = 81°C] was supplied from Shanghai Chemical Engineering Institute (China). Apple odor type essential oil, rosin odor type essential oil, jasmine odor type essential oil, and chrysanthemum odor type essential oil were all made from Tianjin Compound Essence Institute (China).

Preparation of PP/EVA blends

Particles of EVA and PP, previously dried, were placed in an SJ-20 Z×25 plastic extruder in which the spinning jet was equipped with a static mixer to spin through a cool water bath. The tows of PP/EVA blends were then cut into 3-mm-long particles, dried, cooled, and put into the drier to reserve.

SEM of PP/EVA blends

The PP/EVA blends were placed in methylbenzene to sculpt the EVA, broken in liquid nitrogen, and gilded with sputter-coating film equipment. The surface microstructure and cross section of PP/EVA blends were observed with an S450 scanning electron microscope (Hitachi, Ibaraki, Japan).

Thermal behavior measurement

The melting behavior PP/EVA blends was investigated with a Perkin–Elmer DSC-2C differential scanning calorimeter (DSC; Perkin Elmer Cetus Instruments, Norwalk, CT) in a nitrogen atmosphere. An empty sample pan was taken as the reference sample. The samples were cut into small pieces, weighed accurately at 8 ± 0.5 mg, and heated to 500 K at a heating rate of 20 K/min.

Rheological behavior measurement

The rheological behavior of PP/EVA blends was determined by a custom-made rheometer. The draw ratio of the spinneret plate was 5.

Melt spinning of the PP/EVA blends

We spun PP and different compositions of PP/EVA blends, respectively, in a custom-made microplunger-type frame with melt spinning by the extrusion method. The spinneret plate was homogeneous (6 pores; pore diameter, 0.3 mm).

Drawing of matrix fiber

The drawing of as-spun matrix fiber was carried out at a temperature of 95–100°C on a custom-made drawing machine. The drawing ranged from 1.5 to 3.5.

Heat treatment

The drawn matrix fibers were dried and heat-treated at different temperatures for 10 min.

Sorption property of the matrix fiber measurement

We dipped the after-treatment matrix fibers into an essential oil absolute alcohol solution and determined the sorption amount of the matrix fiber for essential oil after a definite time. The sorption amount Γ was calculated from the following equation:

$$\Gamma = (C_0 - C_i)/S \quad (1)$$

where C_0 is the original content of essential oil when the matrix fiber was not dipped into the immersion solution; C_t is the residual content of essential oil when the matrix fiber was dipped into the immersion solution; and S is the surface area of the matrix fibers.

Preparation of the fragrant fiber

The after-treatment matrix fibers were placed into an essential oil absolute alcohol solution or essential oil to adsorb perfume molecules. After adsorption equilibrium, the fibers were taken out, washed, and dried.

RESULTS AND DISCUSSION

Compatibility of PP/EVA

From the macromolecular structure of EVA and PP, we could learn that there were many –(CH_2)– units in EVA and PP macromolecular chains. According to the law of compatibility, PP/EVA had a definite degree of compatibility because of the similarity of methylidynel chains in the two kinds of polymers. Meanwhile, because of the difference of the composition and structure between the –$OCOCH_3$ of EVA and PP main chain, the compatibility of EVA and PP was limited.

It is known from thermodynamics that if the mutual reciprocal of two components was a spontaneous process, the change of the blending free energy ΔG_m must be satisfied with the following:

$$\Delta G_m = \Delta H_m - T\Delta S_m < 0 \quad (2)$$

where ΔG_m is the free energy of blending, ΔH_m is the heat of blending, T is the absolute temperature, and ΔS_m is entropy. Referring to the theory of the macro-

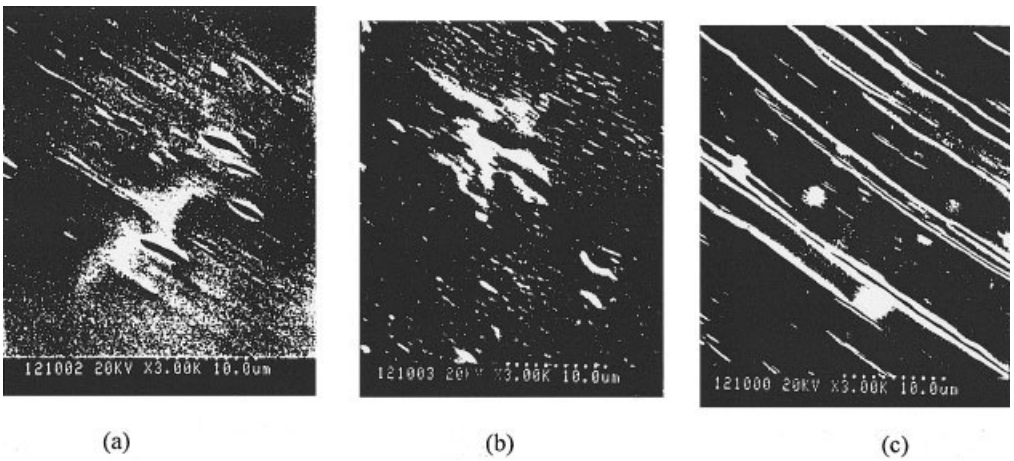

Figure 1 Scanning electron micrographs of surface of PP/EVA blends.

molecular solution's lattice, the conformational entropy of the blending of macromolecules is satisfied with the following:

$$\Delta S_m = -RV/V_r(\Phi_1/x_1 ln\Phi_1 + \Phi_2/x_2 ln\Phi_2) \quad (3)$$

where Φ_1 and Φ_2 are the volume percentage of component 1 and component 2, respectively; V is the volume of blending; V_r is the volume of the chain segment; and x_1 and x_2 are the statistic chain segment number of the two respective components.

Because the molecular weights of the EVA and PP were larger (x was larger), ΔS_m in the blending process was smaller. Obviously, the ΔG_m was determined by ΔH_m. According to the solution's lattice $\Delta H_m \propto (\delta_1 - \delta_2)^2$, where δ_1 and δ_2 are the solubility parameters of the two polymers. Generally, the two polymers were compatible only with extreme difficulty when $|\delta_1 - \delta_2| > 0.5$–1. Referring to the $\delta = \rho \sum F_i/M$, which was advocated by Small,[14] where F_i is the gravitation constant and M is the molecular weight of the polymer segment, we could estimate that the homopolymerization solubility parameter of PP was $\delta_{PP} = 8.04$ (cal $cm^{-3})^{1/2}$. Referring to the random copolymer solubility parameter estimation formula $\delta_c = \sum \delta_c \Phi_i^c$, where Φ is the volume percentage and δ_i is the homopolymerization solubility parameter, which is a composite of the copolymer, we could estimate that the EVA solubility parameter was $\delta_{EVA} = 8.89$ (cal $cm^{-3})^{1/2}$. Because $|\delta_{EVA} - \delta_{PP}| = 0.85$, we learn that EVA and PP are compatible only with the utmost difficulty.

SEM of PP/EVA blends

Figure 1 and Figure 2 are, respectively, scanning electron micrographs of the surface and cross section of the PP/EVA blends with different contents of EVA. From Figure 1 it may be observed that PP/EVA blends are heterogeneous and are characterized by a type of sea-islands structure. In the surface of the PP/EVA blends (EVA content of 5%), EVA exists as a flat and long phase; in the surface of PP/EVA blends (EVA content of 10%), EVA also exists as a flat and long

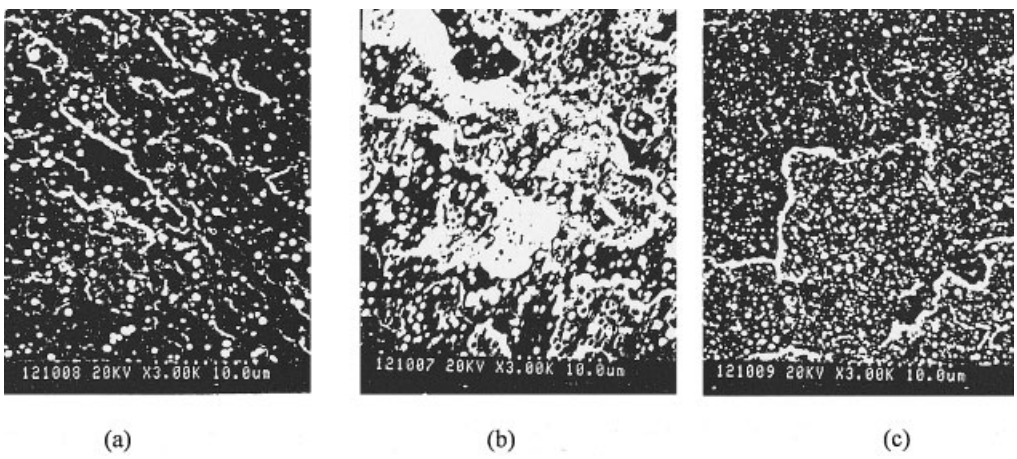

Figure 2 Scanning electron micrographs of cross section of PP/EVA blends.

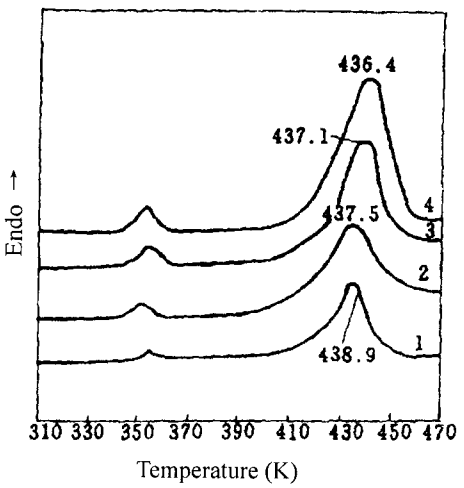

Figure 3 DSC curves of the PP/EVA blends with different EVA content: (1) EVA/PP = 0/100; (2) PPA/EVA = 95/5; (3) PP/EVA = 90/10; (4) PP/EVA = 80/20.

phase. In the surface of PP/EVA blends (EVA content of 20%), EVA existed as a long and thin phase. The number of EVA phases apparently increased with the increase of EVA content. From the SEM of the cross section of PP/EVA blends it may be seen that the EVA phases were well distributed. The area of the EVA circular phases decreased and the number of EVA phases increased successively with the increase of EVA content. EVA was homogeneously distributed in the PP continuous phase as long and thin when the EVA content was low in the PP/EVA blends. With the increase of EVA, the EVA phase deformed and changed from a thick long column to a thin long column. Because the viscoelasticity of EVA was greater than that of PP, PP/EVA blends were apt to deform under the segmentation of the rotary vane of the static mixer when the content of EVA was high.

DSC analysis of the PP/EVA blends

Figure 3 shows the DSC curves of the PP/EVA blends with different EVA contents. From Figure 3 it may be seen that the DSC curve of the PP/EVA is just a composite of the DSC curves of both the PP component and the EVA component, and the addition of EVA did not change the shape of the DSC curve of the PP component. It also shows that EVA could not enter the crystal region of the PP component, and the mixed crystal of PP/EVA did not form when PP/EVA blends crystallized. Table I lists the thermal properties of the PP/EVA blends with different EVA contents. From Table I it may be seen that the crystallizing point of the PP component and the melting point of PP/EVA blends all decreased with the increase of EVA content. It indicates that the addition of EVA could decrease the crystal integrity and the crystal size of the PP component.

TABLE I
Thermal Properties of the PP/EVA Blends with Different EVA Content

PP/EVA (%)	Crystallizing point of PP component (K)	Melting point of PP/EVA blends (K)
100/0	383.36	438.9
95/5	382.90	437.5
90/10	382.88	437.1
80/20	382.44	436.4

Effects of EVA content on the stability of melt spinning of PP/EVA blends

According to rheology theory,[15] the shear flow of fluid that passes through the spinning head and the drawing flow of the spinning thread are the most related to the form of fiber. The two kinds of flow behaviors directly affect the diameter and unevenness, the two factors that affect the flow behaviors. One is an internal cause: composition and structure of the sample; the other is an external cause: spinning temperature, shear speed, winding speed, and the structure of the spinneret.

At present, there are three ways to determine the spinnability[16]: (1) the method to determine the tenuous flow's longest tensile length, (2) the method to determine the tenuous flow's extension at break, and (3) the method to determine the largest drawing ratio. In practice the third method is the most popular one. The largest spinning jet's drawing ratio equals the maximum of the ratio of winding speed to extrusion speed. Table II shows the effect of the EVA content on the spinnability of PP/EVA blends. From Table II it may be seen that at conditions of the same spinning temperature and extrusion speed, with the increase of the EVA content, the maximum winding speed (which could represent the maximum spinning jet ratio) and the time without broken ends (which could represent the tenuous flow's longest tensible elongation) decreased successively. It may be also seen that the spinnability decreased successively with increases of EVA content and the spinnability of the PP/EVA = 80/20 sample was extremely poor.

Changes in apparent viscosity of the PP/EVA blends with EVA content at different temperatures are shown in Figure 4. The viscoelasticity of EVA was

TABLE II
Effects of EVA Content on the Spinnability of PP/EVA Blends

PP/EVA (%)	Spinning temperature (°C)	Maximum winding speed (m/min)
100/0	230	680
95/5	230	620
90/10	230	600
80/20	230	400

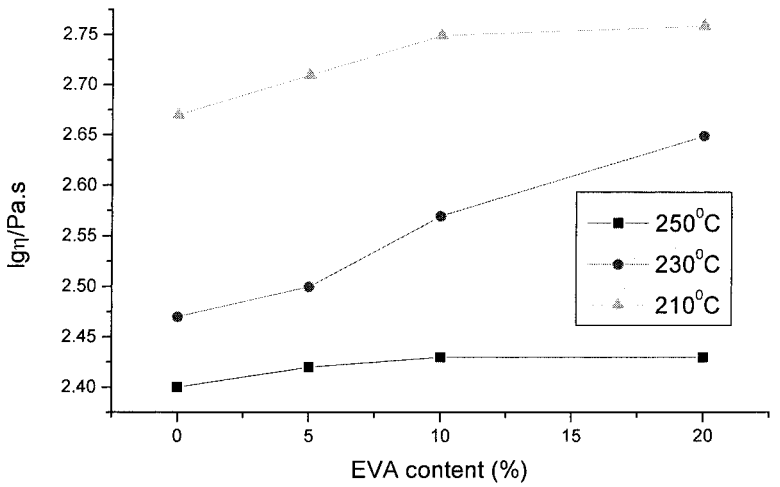

Figure 4 Changes in apparent viscosity of the PP/EVA blends with EVA content at different temperatures.

greater, and EVA had a thickening effect on the PP/EVA blends. From Figure 4, it may be seen that when EVA was added to PP, the apparent viscosity of PP/EVA blends increased with the increase of EVA content. The flow curves of PP/EVA blends with 10% EVA are shown in Figure 5. From Figure 5 it may be seen that the PP/EVA blend was a typical pseudoplastic fluid. At a certain temperature, we could lower the apparent viscosity of the melt of PP/EVA blends and improve the spinnability by increasing the shear speed. However, the shear speed could not be endlessly increased. At a constant spinnable temperature the shear speed did not reach a fixed value, until the melting blend would burst. The fixed speed was the critical shear speed at the temperature of this system, and apparently the critical shear speed of the PP/EVA blend decreased with an increase of the EVA content. Because the elasticity of EVA was greater than that of PP, the normal pressure difference caused by the melting blend flowing in the spinning jet would be increased, and the orientation macromolecule's swelling phenomenon was exacerbated at the equipment's outlet.

Effect of spinning temperature on the stability of melt spinning of PP/EVA blends

Changes in spinnability of the PP/EVA blends with spinning temperature are shown in Table III. At a definite extrusion speed and at 230°C, the winding speeds of PP/EVA blends with different EVA contents were the highest and their broken ends numbered the least at the same time. We could observe broken capillaries at 260°C. Below 210°C, the melt fracture phenomena all appeared with different degrees. Under all experimental conditions, the spinnability of PP/EVA blend was the best at 230°C. From Figure 4, we learn that the apparent viscosity of PP and melting blends all decreased with the increase of the spinning temperature. With the increase of the temperature, the

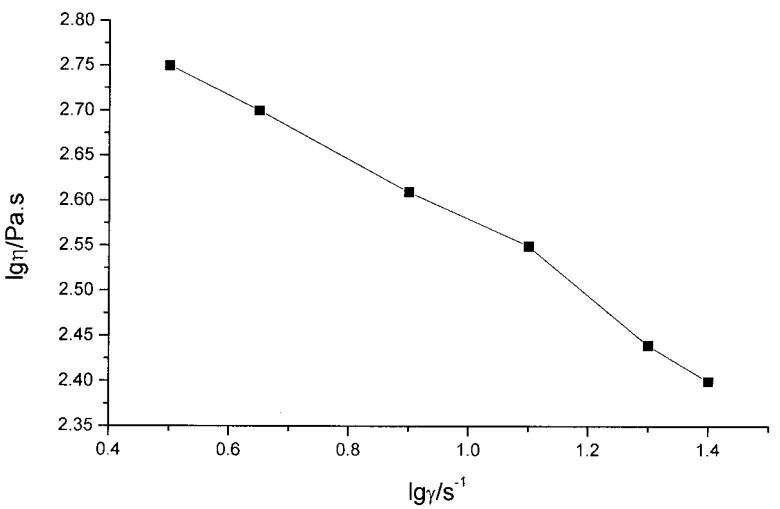

Figure 5 Flow curve of PP/EVA blends with 10% EVA.

TABLE III
Changes in the Spinnability of PP/EVA Blends with Spinning Temperature

PP/EVA (%)	Spinning temperature (°C)	Maximum winding speed (m/min)
95/5	210	600
	230	630
	260	540
90/10	210	500
	230	630
	260	500
80/20	210	300
	230	400
	260	300

free volume of the melting blend increased. It was apt to move for the macromolecule's chains, to disentangle the macromolecular segments, and cause a decrease in apparent viscosity. The flowability of melting blends could be improved by increasing the temperature, but too high a temperature could cause an adverse by-reaction to appear and also affect the spinning stability and property of fiber formation. When the spinning temperature was too low, the viscosity of PP/EVA blends would increase. When the elastic density caused by stress surpassed the cohesive energy density, the cohesive failure would occur and the spinnability of the blends would become poor; when the spinning temperature was too high, the viscosity of melting blends was too low, winding and drawing would make the fiber's fluctuation expand and cause broken capillaries, and the spinnability would become poor. Thus it is vital to establish a suitable spinning temperature region in the melt-spinning process.

Effect of the match between pump delivery and winding speed on the melt-spinning stability

In general the as-spun fiber reached the ultimate diameter away from the spinneret plate about 0.3–0.5 cm. It meant that in a brief time the melt blend left the spinneret plate and the spin axial velocity gradient had reached the maximum. The velocity gradient was the primary reason that the fiber could generate stretching resistance. Within a brief time the tremendous drawing ratio and larger velocity gradient caused the stretching resistance of fiber to incline to the limit of the single-fiber's tensile strength. In addition, there were some EVA phases that had greater viscoelasticity in the melt PP/EVA blend; thus it could change the macromolecular interreaction to a certain degree. If we were slightly incautious in the control of spinning process, broken ends would probably appear and a continuous fiber could thus not be spun. This was just the difficulty in the spinning process when EVA was added to the PP. The shear speed of the melting blend in the spinneret orifice was directly related to the extrusion speed. The drawing rate was the ratio of pump delivery to winding speed. Thus it was more significant to consider comprehensively both pump delivery and winding speed in the spinning process. Table IV shows the relationship between the different matches of pump delivery to winding speed and spinning stability at a certain spinning temperature and spinneret orifice diameter. From Table IV it may be seen that when the ratio of pump delivery to winding speed was 70/500, both the PP/EVA = 90/10 and PP/EVA = 95/5 samples were successively spinnable for 30 min, broken ends numbered the least, and the spinning stability was good. When the ratio of pump delivery to winding speed was 70/400 the sample with EVA content of 20% had longer spinning time and the spinning stability was better. Above all, the match of pump delivery to winding speed significantly affected the stability of PP/EVA melt spinning.

Sorption properties of the matrix fiber for different essential oils

Changes in the adsorption amount of matrix fiber for different essential oils (apple odor type essential oil, rosin odor type essential oil, jasmine odor type essential oil, and chrysanthemum odor type essential oil)

TABLE IV
Effects of the Match Between Pump Delivery and Winding Speed on the Spinnability of PP/EVA Blends

PP/EVA (%)	Pump delivery (g/min)	Winding speed (m/min)	Spinning time (min)	Spinnability
95/5	50	500	25	good
95/5	70	500	30	very good
95/5	100	500	26	good
90/10	50	500	24	good
90/10	70	500	32	very good
90/10	100	500	24	good
80/20	50	400	15	bad
80/20	70	400	30	very good
80/20	100	400	2	bad

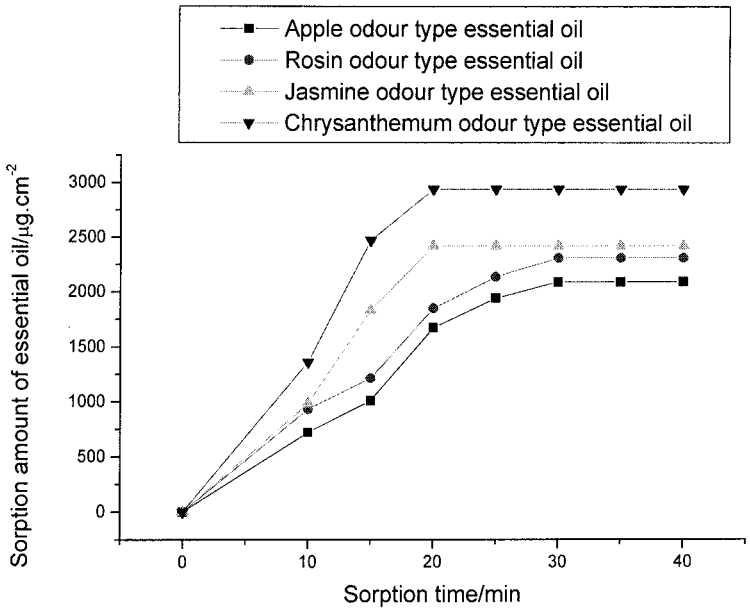

Figure 6 Plot of sorption amount of matrix fiber for different essential oils versus sorption time. Conditions: EVA content, 10%; essential oil mass fraction, 12%.

with sorption time are shown in Figure 6. From Figure 6 it may be seen that the sorption amount of essential oil would not change after 30 min. This shows that the adsorption speed of the matrix fiber was fast for essential oil, and it was related to the morphological structure of the matrix fiber. When the sorption time reached 30 min, the EVA had completely reacted, the sorption had been saturated, and the sorption amount no longer changed with time.

Changes in sorption amount of matrix fiber for essential oil with EVA content at the same temperature and the same time are shown in Figure 7. From Figure 7 we learn that the adsorption amount of matrix fiber for essential oil apparently increased with the increase of the EVA content. This illustrates that the adsorption amount of matrix fiber mainly depended on the effective EVA content that contained the adsorption-active sites. Experiments in which the matrix fiber adsorbed essential oil in the same time and at the same temperature were also carried out. The results showed that the adsorption amounts of the matrix fiber for chrysanthemum odor type essential oil and jasmine odor

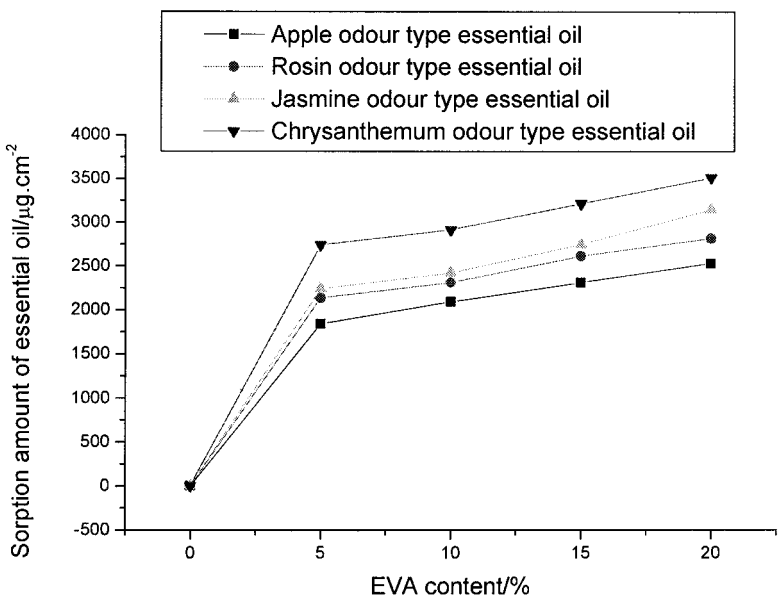

Figure 7 Effect of EVA content on the sorption amount of matrix fiber for different essential oils. Conditions: Sorption time, 30 min; essential oil mass fraction, 12%.

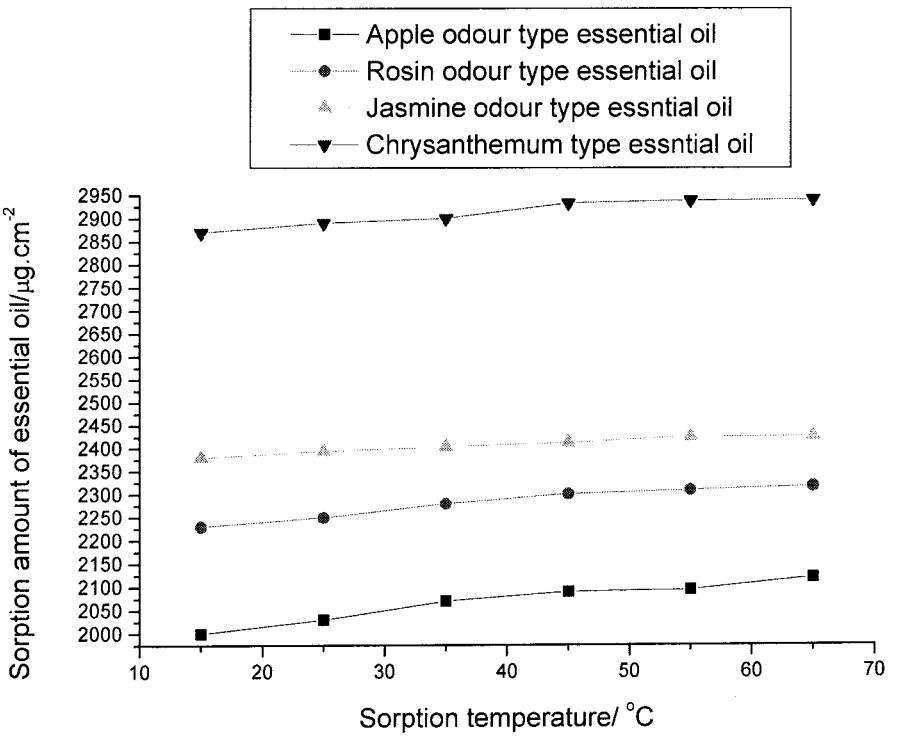

Figure 8 Plot of sorption amount of matrix fiber for different essential oils versus temperature. Conditions: EVA content, 10%; essential oil mass fraction, 12%; sorption time, 30 min.

type essential oil were greater than the adsorption amounts of matrix fiber for apple odor type essential oil and rosin odor type essential oil. It was related to the chemical structure of the four kinds of essential oil.

Changes in the adsorption amounts of essential oil into matrix fiber with adsorption temperature in the same time are shown in Figure 8. From Figure 8 we learn that the adsorption amount of essential oil into the matrix fiber was fundamentally identical at 15–55°C, which illustrates that the adsorption activation energy of matrix fiber for essential oil was lesser according to the Arrhenius equation.

Essential oil and absolute alcohol formed a binary liquid phase mixture. We must take into consideration the effects among adsorbent (matrix fiber), solute (essential oil), solvent (absolute alcohol), and the boundary surface oriented molecules when matrix fiber adsorbs essential oil from the binary liquid phase mixture. The adsorption amount of solution was generally calculated according to the change of one component after adsorption. In fact the adsorption amount constitutes both a relative adsorption amount and an apparent adsorption amount: it was an excess in essence. Figure 9 shows the composite isotherms of the apparent adsorption of matrix fiber for essential oil alcohol solution. In fact, the apparent isotherm of the adsorption represents the composite results of the single isothermal curve of essential oil and the single isothermal curve of alcohol, so it was also called a composite isotherm. Generally, there were two kinds of composite isotherms of adsorption: one was a *U*-type composite isotherm; the other, an *S*-type composite isotherm. From Figure 9 it may be seen that the composite isotherm of the adsorption of matrix fiber for essential oil was characteristic of a *U*-type model. The maximum occurred in the curve. There have been some reports[17] that the *U*-type model composite isotherm could generally be divided into single isothermal curves and the monolayer adsorption model was generally used. We could infer the single adsorption isothermal curve of the matrix fiber for essential oil-alcohol binary liquid phase mixture with this model. With the increase of essential oil mass fraction, the single adsorption amount of the matrix fiber for essential oil increased, but the adsorption amount of the matrix fiber for alcohol decreased. If the adsorption were multilayer in nature, there would be still no way at present to divide the composite isotherm of the adsorption into single isothermal curves.

Preparation technique of immersion-type fragrant fiber

The matrix fiber adsorbed essential oil through the fiber micropores and the essential oil molecules were bound to the active site on the inner surface of the fiber. In this process the essential oil molecules were adsorbed by the matrix fiber with the help of the essential oil affinity in the fiber because of the chemical potential difference of the essential oil molecules

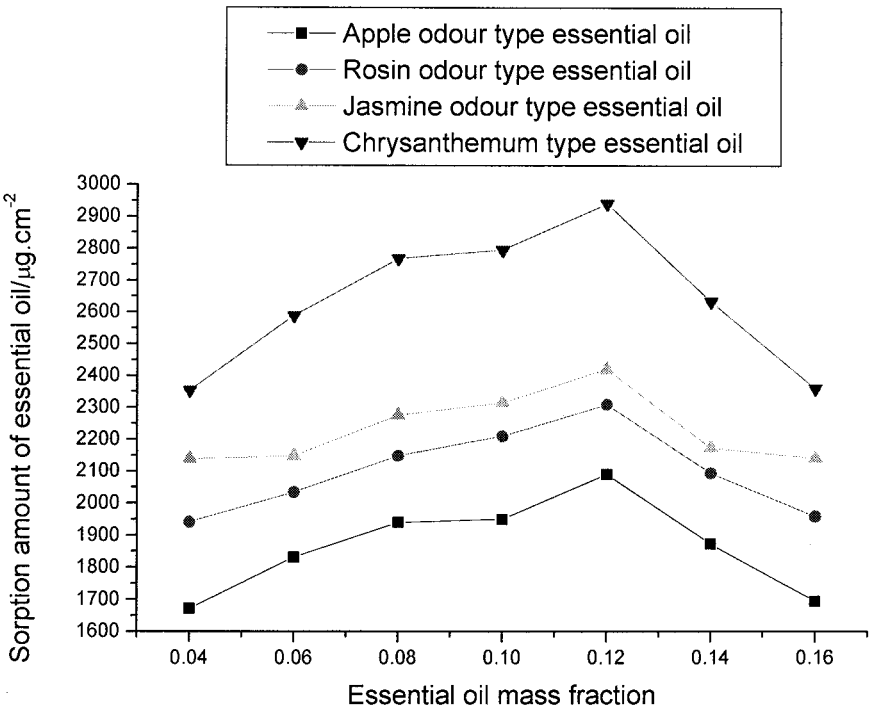

Figure 9 Composite adsorption isotherms of matrix fiber for different essential oils. Conditions: EVA content, 10%; sorption time, 30 min.

between the solution and the matrix fiber. The matrix fiber was the heterogeneous melt-spun fiber and had the matrix–microfiber structure. The dispersion-phase EVA was a slender body and homogeneous. The boundary surface between the EVA phase and the PP phase was looser because of the poor compatibility between EVA and PP. Some slack-type imperfections appeared between the two phases. The structure of the matrix fiber allowed the essential oil molecules greater passage and thus to be more easily adsorbed, diffused, and stored. From the chemical structure it may be seen that the ester groups on the side chains of EVA macromolecules, the lateral group of EVA, formed affinity-active sites for essential oil molecules. With the help of the weak hydrogen bond between essential oil molecules and carboxide, the dipole force and van der Waals force, the matrix fiber adsorbed the essential oil molecules. The matrix fibers were immersed into the essential oil absolute alcohol solution or essential oil to adsorb perfume molecules. After adsorption equilibrium, the fibers were removed, washed, and dried to become immersion-type fragrant fibers. The immersion-type fragrant fibers were maintained for 1 year to adjust their fragrance properties. The experiment showed that the fragrance properties of the chrysanthemum odor type fragrant fiber was very good, the fragrance properties of the jasmine odor type fragrant fiber was good, and the fragrance properties of the apple and rosin odor type fragrant fibers were generally not remarkable.

CONCLUSIONS

The PP/EVA blends were thermodynamically incompatible and had typical sea-island structures. The second component EVA could affect both the melting point and the crystal temperature of PP. PP and EVA crystallized, respectively, and did not form mixed crystals in the blends. In this experiment the PP/EVA $< 80/20$ blends were characterized by good spinnability. EVA as the dispersed phase caused the spinnability of PP/EVA blends to decrease. Under strictly controlled spinning process conditions, PP/EVA blends could be spun into a definite diameter and well-distributed matrix fiber of the fragrant fiber. The matrix fibers could adsorb essential oil to become immersion-type fragrant fibers that had good fragrance properties.

References

1. Wakahara, H.; Tagawa, K. Jpn. Kokai Tokkyo Koho JP 02, 182,980 [90,182,980].
2. Yoshihara, M.; Kawakita, M.; Yamahara, M. Korgo 1990, 167, 53 (in Japanese).
3. Wakahara, H.; Tagawa, K. Jpn. Kokai Tokkyo Koho JP 02, 200,876 [90,200,876].
4. Ichinose, N.; Suzuki, S. Jpn. Kokai Tokkyo Koho JP 02, 202,997 [90,202,997].
5. Wakahara, H.; Tagawa, K.; Nanoo, T. Jpn. Kokai Tokkyo Koho JP 02, 185, 256 [90,185,256].
6. Makino, S.; Ito, A. Jpn. Kokai Tokkyo Koho JP 02, 221,468 [90,221,468].

7. Kobayashi, S. Jpn. Kokai Tokkyo Koho JP 2001 62, 828 (Cl. B29B7/94).
8. Dittmar, R. M.; Chao, T. L.; Palmer, R. A. Appl Spectrosc 1991, 45, 1104.
9. Garcia, J. F.; Shih, J. Eur. Pat. Appl. EP 426,346.
10. Dollinger, H. M.; Sawan, S. P. Polymer Drug Delivery Systems; ACS Symposium Series 469; American Chemical Society: Washington, DC, 1991; pp. 181–193.
11. Vargas do Amaral, J. S. Braz. Pedido PI BR 89 06, 461.
12. Smith, T. N. Chem Eng Res Des 1991, 69, 398.
13. Imaizumi, M.; Kuriyama, M.; Takeuchi, T. Jpn. Kokai Tokkyo Koho JP 03 27,937 [91 27,937].
14. Tadokoro, H. Structure of Crystalline Polymers; Wiley-Interscience: New York, 1979; p. 358.
15. Macsko, C. W. Rheology Principles, Measurement, and Application; VCH: New York, 1994; Chapter 4.
16. Tadmor, Z.; Gogos, C. G. Principles of Polymer Processing; Wiley: New York, 1979; Chapter 6.
17. Kinling, J. J. Adsorption from Solution of Non-Electrolytes; Academic Press: London and New York, 1965.